Cell, Vol. 122, 593–603, August 26, 2005, Copyright ©2005 by Elsevier Inc. DOI 10.1016/j.cell.2005.06.014

Proapoptotic BID Is an ATM Effector in the DNA-Damage Response

Iris Kamer,[1,4] Rachel Sarig,[1,4] Yehudit Zaltsman,[1] Hagit Niv,[1] Galia Oberkovitz,[1] Limor Regev,[1] Gal Haimovich,[1] Yaniv Lerenthal,[2] Richard C. Marcellus,[3] and Atan Gross[1,*]

[1]Department of Biological Regulation
Weizmann Institute of Science
Rehovot 76100
Israel

[2]Department of Human Genetics
Sackler School of Medicine
Tel Aviv University
Tel Aviv 69978
Israel

[3]Geminx Biotechnologies Inc.
Place du Parc, Montreal, Quebec H2W 2M9
Canada

Summary

The "BH3-only" proapoptotic BCL-2 family members are sentinels of intracellular damage. Here, we demonstrated that the BH3-only BID protein partially localizes to the nucleus in healthy cells, is important for apoptosis induced by DNA damage, and is phosphorylated following induction of double-strand breaks in DNA. We also found that BID phosphorylation is mediated by the ATM kinase and occurs in mouse BID on two ATM consensus sites. Interestingly, *BID*$^{-/-}$ cells failed to accumulate in the S phase of the cell cycle following treatment with the topoisomerase II poison etoposide; reintroducing wild-type BID restored accumulation. In contrast, introducing a nonphosphorylatable BID mutant did not restore accumulation in the S phase and resulted in an increase in cellular sensitivity to etoposide-induced apoptosis. These results implicate BID as an ATM effector and raise the possibility that proapoptotic BID may also play a prosurvival role important for S phase arrest.

Introduction

The BH3-only proteins are sentinels of intracellular damage (Puthalakath and Strasser, 2002). These proteins are held in check by diverse mechanisms, seemingly at cellular locations at which they can sense specific damage.

BID is believed to be relatively inactive in the cytosol until proteolytically cleaved by caspase-8. Cleavage of cytosolic BID at Asp59 yields a p15 C-terminal truncated fragment (tBID) that translocates to the mitochondria, where it induces the activation of BAX and BAK, resulting in the release of cytochrome c (Wang, 2001). Phosphorylation seems to regulate BID activity, since it was recently demonstrated that its phosphorylation by casein kinase 1 and/or 2 inhibits its cleavage by caspase-8 (Desagher et al., 2001).

However, the apoptotic pathways in which BID plays a role are not yet fully characterized. Studies with *BID*$^{-/-}$ mice have demonstrated that BID is required for Fas-induced apoptosis (Yin et al., 1999). On the other hand, *BID*$^{-/-}$ mouse embryonic fibroblasts (MEFs) were found to be as susceptible as *BID*$^{+/+}$ MEFs to a wide range of intrinsic damage signals (Wei et al., 2001). More recently, however, it was demonstrated that *BID*$^{-/-}$ MEFs are less susceptible than *BID*$^{+/+}$ MEFs to the DNA-damage reagent adriamycin, as well as to the nucleotide analog 5-fluorouracil (Sax et al., 2002). Thus, BID may contribute to the DNA-damage response.

In eukaryotes, each cell's genetic material is constantly subjected to DNA damage. While a double-strand break (DSB) is not the major DNA lesion, it is certainly among the most harmful. Following DSBs, the cell may activate a survival system that enables repair and continuation of its normal life cycle, or it may activate its apoptotic machinery in the face of extensive or irreparable damage (Kaina, 2003).

One of the major responses associated with the cell-survival network is the temporary arrest of cell cycle progression, which reflects the activation of cell cycle checkpoints (Iliakis et al., 2003). The best-documented, damage-induced cell cycle checkpoints operate in the G_1/S boundary and at the S and G_2 phases. The very early events that take place at the site of a DNA double-strand break and precede activation of the response network involve several proteins that are rapidly recruited to the damaged site; there, they act as DSB sensors. They then convey a damage signal to transducers, which in turn deliver it to numerous downstream effectors.

A prototype transducer of the DSB response is ATM, a nuclear serine-threonine protein kinase which is absent or inactivated in patients with the genomic instability syndrome ataxia-telangiectasia (A-T) (Shiloh, 2003). Cells from A-T patients exhibit genomic instability, radiosensitivity, and defective activation of the entire DSB response, most notably, the cell cycle checkpoints. ATM is a member of a group of conserved large proteins, several of which are protein kinases involved in mediating DNA-damage responses. These proteins (including ATR [ATM and RAD3-related]) share several motifs, among them a domain containing a PI3-kinase signature, which gives this group the title, "PI3-kinase-related protein kinases" (PIKKs). Activated ATM phosphorylates a wide spectrum of substrates, many of them at the sites of damage. The functional consequences of some of ATM phosphorylation events have been associated with the activation of the cell cycle checkpoints. However, not all of the phenotypic abnormalities in A-T patients and their cells can be explained by a lack of these phosphorylation events, implying that additional ATM targets exist, which have not yet been identified.

Previously, we suggested that full-length BID is a player in the DNA-damage pathway, since a caspase-8

*Correspondence: atan.gross@weizmann.ac.il
[4]These authors contributed equally to this work.

noncleavable BID mutant sensitized *BID*$^{-/-}$ mouse embryonic fibroblasts (MEFs) to DNA damage-induced apoptosis (Sarig et al., 2003). Our current findings demonstrate that BID is partially localized to the nucleus in healthy MEFs and is important for apoptosis induced by a variety of DNA-damaging reagents. Moreover, we show that etoposide and ionizing radiation, both of which are known to induce double-strand breaks in DNA, lead to the phosphorylation of BID. Our findings indicate that BID phosphorylation is mediated by the ATM kinase, and occurs in mouse BID on two ATM consensus sites ($S^{61}Q$ and $S^{78}Q$). We also found that etoposide induced accumulation of *BID*$^{+/+}$ MEFs in the S and G_2 phases of the cell cycle, whereas such an accumulation was not observed in the *BID*$^{-/-}$ MEFs. Reintroducing wild-type BID into *BID*$^{-/-}$ cells restored their ability to accumulate in the S and G_2 phases, whereas introducing a nonphosphorylatable BID mutant (S61A/S78A) restored accumulation in the G_2 phase but not in the S phase. Moreover, in response to etoposide, the mutant BID cells entered apoptosis more readily than did the wild-type BID cells. These results implicate BID as an ATM effector and raise the novel possibility that BID, a molecule that was previously considered to be active only as a proapoptotic factor, may also play a prosurvival role important for S phase arrest.

Results

BID Is Important for DNA Damage-Induced Apoptosis

To determine whether BID is required for DNA damage-induced apoptosis, we generated hTERT-immortalized *BID*$^{+/+}$ and *BID*$^{-/-}$ mouse embryonic fibroblasts and analyzed their response to a variety of DNA-damaging reagents: etoposide (Etop; a specific inhibitor of topoisomerase II), cisplatin (*Cis*; forms covalent adducts with the DNA), ultraviolet radiation (UV; induces thymine dimers), and ionizing radiation (IR). We found that *BID*$^{-/-}$ MEFs were less susceptible than *BID*$^{+/+}$ MEFs to all four treatments (Figure 1A). These DNA-damaging reagents also induced less cell death in primary *BID*$^{-/-}$ MEFs than in primary *BID*$^{+/+}$ MEFs (data not shown), confirming that this decreased sensitivity is not due to hTERT immortalization. Splenocytes from *BID*$^{-/-}$ mice also display less susceptibility to Etop treatment (see Figure S1A in the Supplemental Data available with this article online), indicating that the decreased death response to DNA damage is a general feature of BID deficiency, although it is more pronounced in MEFs.

To confirm that *BID*$^{-/-}$ MEFs are indeed less sensitive than *BID*$^{+/+}$ MEFs to DNA damage-induced cell death, we performed clonogenic survival assays with MEFs following DNA damage. Our studies show that *BID*$^{-/-}$ MEFs have increased clonogenic survival following IR and Etop treatment (Figure 1B and data not shown). We have also created MEFs that are more sensitive to DNA damage-induced cell death by transforming primary *BID*$^{+/+}$ and *BID*$^{-/-}$ MEFs with the SV40 whole genome. Cell death assays with these cells using much lower levels of DNA-damaging reagents confirmed that BID loss reduces sensitivity to DNA damage-induced cell death (Figure S1B). Finally, to confirm that the reduced susceptibility of *BID*$^{-/-}$ MEFs to DNA-damaging reagents was due to the absence of BID, *BID*$^{-/-}$ MEFs were infected with recombinant adenoviruses carrying the BID vector prior to treatment with Etop or IR. The results show that reintroduction of BID did not induce cell death on its own but fully restored susceptibility to Etop- (and partially to IR)-induced cell death (Figure 1C).

DNA-Damaging Reagents Causing Double-Strand Breaks Induce the Phosphorylation of BID, and This Phosphorylation Is Mediated by the ATM Kinase

Next, we explored whether BID was modified in response to DNA damage. Western blot analysis using anti-BID antibodies on lysates of hTERT-immortalized *BID*$^{+/+}$ MEFs treated with the DNA-damaging reagents mentioned above revealed that Etop and IR, which are known to induce DSBs in DNA, unlike *Cis* or UV, induced a double electrophoretic mobility shift in BID (Figure 2A, note that the lower of the two shifted bands does not separate well from the regular BID band). We also treated MEFs with several other apoptotic reagents: thapsigargin (Thaps; stress signaling from the ER, which inhibits the Ca^{2+} adenosine triphosphate pump); TNFα together with actinomycin D; or with staurosporine (STS; a kinase inhibitor) and found that none of them affected the electrophoretic mobility of BID (Figure 2A). Etop and IR induced a similar double electrophoretic mobility shift in BID also in primary *BID*$^{+/+}$ MEFs (data not shown), confirming that this shift is not due to hTERT immortalization. Similar mobility shifts have been associated with covalent modifications of proteins, for example, as a consequence of phosphorylation.

To define whether the double electrophoretic mobility shift in BID was due to phosphorylation, *BID*$^{+/+}$ MEFs were treated with Etop for 30 min, lysed, and either left untreated or incubated with alkaline phosphatase for 30 min at 37°C. Western blot analysis using anti-BID antibodies demonstrated that treatment with alkaline phosphatase abolished the electrophoretic mobility shifts in BID (Figure 2B), indicating that these shifts are most likely due to phosphorylation. Taken together, these results strongly suggest that BID is rapidly phosphorylated in response to reagents that induce double-strand breaks in DNA.

To confirm that BID was phosphorylated, human cervical adenocarcinoma (HeLa) cells were transfected with mouse BID, labeled with ^{32}P-orthophosphate, either left untreated or treated with Etop, and BID-immunoprecipitated. Exposure to Etop resulted in a marked increase in ^{32}P-labeling of BID, which appeared as a doublet (Figure 2C, left). Western blot analysis of the same samples with anti-BID antibodies indicated that the two ^{32}P-labeled bands correspond to the two slower-migrating forms of BID (Figure 2C, right).

The ATM kinase plays a pivotal role in the immediate response of cells to double-strand breaks. To determine whether ATM is involved in the phosphorylation of BID, we utilized mouse embryonic fibroblasts deficient in both *ATM* and the *p19ARF* tumor-suppressor gene, since loss of *ARF* has been shown to reverse premature replicative arrest of *ATM*-deficient MEFs (Kamijo et al., 1999). Accordingly, *ATM*/*ARF* double-knockout MEFs,

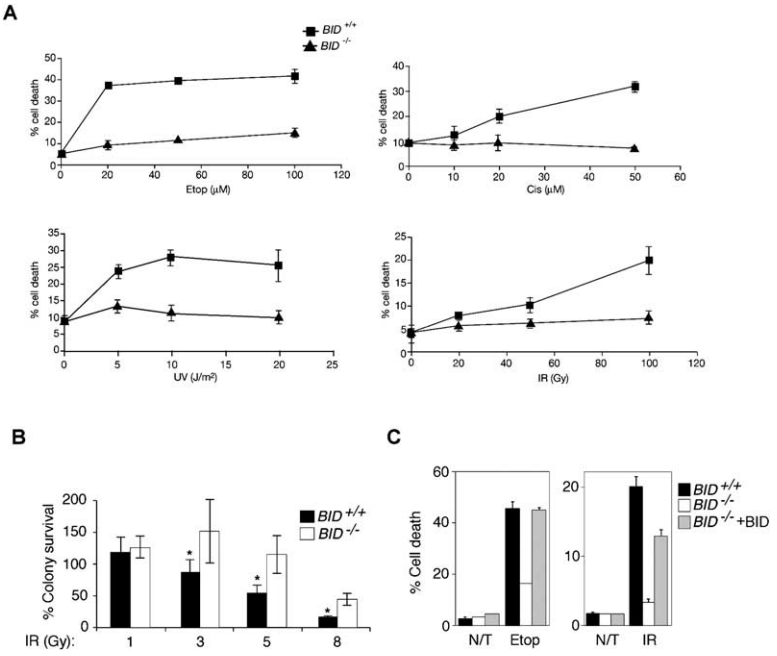

Figure 1. BID Is Important for DNA Damage-Induced Apoptosis

(A) *BID*$^{-/-}$ MEFs are less susceptible than *BID*$^{+/+}$ MEFs to apoptosis induced by DNA-damaging reagents. Dose-response/death curves of *BID*$^{+/+}$ and *BID*$^{-/-}$ MEFs in response to treatment with the indicated doses of Etop (24 hr), *Cis* (14 hr), UV (14 hr), and IR (24 hr). Cell death was monitored by FACScan using PI dye exclusion, as described in the Experimental Procedures. The data shown represent the means ±SEM of pooled results from three independent experiments.

(B) *BID*$^{-/-}$ MEFs have increased clonogenic survival compared to *BID*$^{+/+}$ cells following DNA damage. One thousand cells from *BID*$^{+/+}$ and *BID*$^{-/-}$ MEFs were seeded per well and irradiated with the indicated doses of IR. Cells were then incubated for 10 days and the percent of colony survival was calculated as the ratio of the number of colonies formed after IR to the number of colonies formed in untreated cells. * represent significant differences ($p < 0.05$) based on Student's t test.

(C) The reduced susceptibility of *BID*$^{-/-}$ MEFs to DNA-damaging reagents is due to the absence of BID. *BID*$^{+/+}$ or *BID*$^{-/-}$ MEFs were either left untreated (N/T) or treated with either Etop (100 μM; 24 hr; left) or ionizing radiation (IR; 100 Gy; 24 hr; right), and cell death was monitored by FACScan using PI dye exclusion. Alternatively, *BID*$^{-/-}$ MEFs were infected with recombinant adenoviruses carrying a tetracycline-inducible BID vector. Two hours after the addition of doxycyclin, the cultures were washed three times and treated with either Etop or IR. Cell death was monitored as described above. The data represent the means ±SEM of pooled results from three independent experiments.

as well as *Atm*$^{+/+}$*Arf*$^{-/-}$ MEFs, were treated with Etop or IR and Western blot analyzed using anti-BID antibodies. Figure 2D shows that following Etop or IR treatment, the slower migrating bands of BID do not appear in the *ATM*-deficient cells. Thus, the presence of the ATM kinase appears to play an essential role in the process by which etoposide and ionizing radiation induce phosphorylation of BID.

To corroborate these findings, we took advantage of a stable HeLa cell line in which ATM was knocked down by siRNA (in these cells, the level of ATM was reduced by ~95% [Elkon et al., 2005]). Both these cells and the control cells, which carried a siRNA against LacZ, were transfected with mouse BID, exposed to Etop, and Western blot analyzed using anti-BID antibodies. Exposure of control HeLa cells to Etop induced a double electrophoretic mobility shift in BID that was absent in the ATM knocked-down cells (Figure 2E, left and middle panels). *BID*$^{-/-}$ MEFs were used as a specificity control (Figure 2E, right panel). These results further confirm that the presence of ATM is essential for BID phosphorylation.

Mouse and Human BID Are Phosphorylated on PIKK Consensus Sites

As mentioned in the Introduction, ATM is a member of the PIKK family. The common phosphorylation sites for PIKKs are serines or threonines followed by glutamine residues, a motif commonly dubbed "SQ/TQ" (Kim et al., 1999). Mouse BID carries two such motifs ($S^{61}Q$ and $S^{78}Q$), whereas human and rat BID carry only one ($S^{78}Q$; Figure 3A).

To determine whether mouse BID is phosphorylated on one or both of these sites, we mutated each of these serines to alanines. Our initial analysis was performed in HeLa cells transfected with either wild-type (wt) BID or transfected with one or the other of the BID mutants. Western blot analysis using anti-BID antibodies indicated that treatment of the aforementioned cells with Etop resulted in a double electrophoretic mobility shift, which was abolished in the S61A mutant (Figure 3B). In contrast, mutating the S78 site had no effect on the appearance of the two slower-migrating bands. Thus, BID phosphorylation on S61 is likely the cause for the electrophoretic mobility shift.

To confirm the results presented above and to establish whether serine 78 is also phosphorylated in mouse BID in response to Etop, we generated phosphospecific antibodies to serine 61 and serine 78 (see Experimental Procedures). We initially performed Western blot analysis with these antibodies on lysates of mouse embryonic fibroblasts. To define whether these antibodies recognize the phosphorylated form of BID, *BID*$^{+/+}$ MEFs were either not treated or treated with Etop for 30 min, lysed, and either left untreated or incubated with potato-acid phosphatase for 30 min at 37°C. Western blot analysis demonstrated that anti-pS61 antibodies recognized a band of the expected size of BID in Etop-treated cells and that treatment with potato-acid phosphatase abolished this recognition (Figure 3C, left; note that these antibodies recognize an additional ~30 kDa protein that shares antigenicity with pS61-BID). Western blot analysis using the anti-pS78 antibodies demonstrated that these antibodies recognized three bands (one strong band and two very faint bands) in Etop-treated cells; treatment with potato-acid phos-

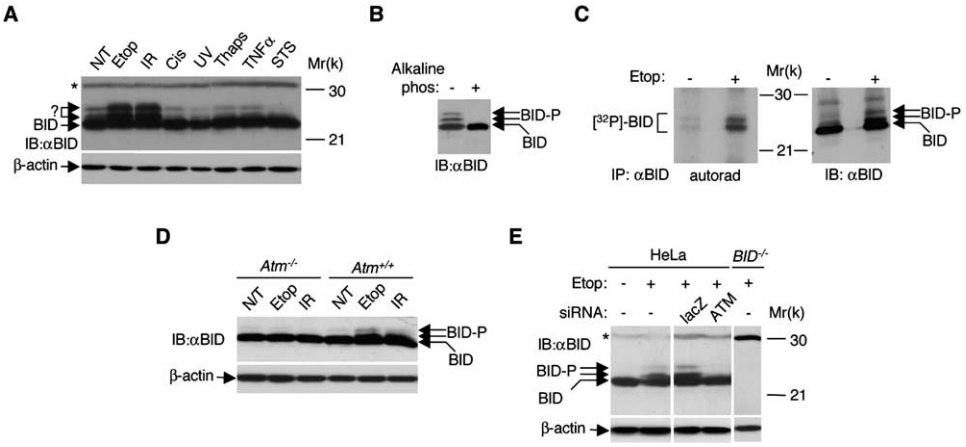

Figure 2. DNA-Damaging Reagents Causing Double-Strand Breaks Induce the Phosphorylation of BID, and This Phosphorylation Is Mediated by the ATM Kinase

(A) Etop and IR induce a double electrophoretic mobility shift in BID. *BID*$^{+/+}$ MEFs were either left untreated (N/T) or treated with one of the indicated cell death stimuli: Etop (100 μM), IR (50 Gy), *Cis* (50 μM), UV (20 J/m^2), Thaps (2 mM), TNFα (40 ng/ml together with 2 μg/ml actinomycin D), and STS (4 μM). Cells were collected 1 hr later, lysed, and equal amounts of protein (20 μg per lane) were subjected to SDS-PAGE, followed by Western blot analysis using anti-BID Abs. The blot was stripped and reprobed with anti-β-actin Abs to control for loading (lower panel). * marks a crossreactive band. The question mark marks the BID double electrophoretic mobility shift.

(B) Alkaline phosphatase treatment abolishes the Etop-induced double electrophoretic mobility shift in BID. *BID*$^{+/+}$ MEFs were treated with 100 μM Etop for 30 min, lysed, and either left untreated (–), or treated with alkaline phosphatase (+) for 30 min at 37°C, followed by Western blot analysis using anti-BID Abs. BID-P marks the BID double electrophoretic mobility shift.

(C) Exposure to Etop results in a marked increase in ^{32}P-labeling of BID, which appears as a doublet. HeLa cells were transiently transfected with pcDNAIII-wtBID. Eighteen hours posttransfection, cells were metabolically labeled with ^{32}P-orthophosphate and later, either left untreated (–), or treated with 100 μM Etop for 30 min. Radiolabeled BID was immunoprecipitated with anti-BID Abs and evaluated by either autoradiography (left) or by Western blot, using anti-BID Abs (right).

(D) The slower-migrating forms of BID do not appear in *ATM*-deficient MEFs. *ATM/ARF* double-knockout MEFs (*Atm*$^{-/-}$) and *Atm*$^{+/+}$*Arf*$^{-/-}$ MEFs (*Atm*$^{+/+}$) were either left untreated (N/T) or treated with 100 μM Etop or 50 Gy IR, collected after 30 min, and lysed. Equal amounts of protein (20 μg per lane) were subjected to SDS-PAGE, followed by Western blot analysis using anti-BID Abs. The blot was stripped and reprobed with anti-β-actin Abs to control for loading (lower panel).

(E) Etop-induced phosphorylation of exogenous BID is detected in LacZ, but not in ATM knocked-down HeLa cells. Left panel: HeLa cells were transiently transfected with pcDNAIII-wtBID. Eighteen hours posttransfection, cells were either left untreated (–) or treated with 100 μM Etop for 30 min, collected, lysed, and Western blot analyzed using anti-BID Abs. Middle panel: stable LacZ knocked-down and stable ATM knocked-down HeLa cells were transfected with pcDNAIII-wtBID, treated with Etop, and analyzed as described for the left panel. Right panel: *BID*$^{-/-}$ MEFs treated with Etop for 30 min were used as a specificity control for the anti-BID Abs. All blots shown in (E) were stripped and reprobed with anti-β-actin Abs to control for loading (lower panels).

phatase abolished all three bands (Figure 3C, right). The bands identified with both antibodies corresponded to BID, since they were not identified in *BID*$^{-/-}$ MEFs (Figure 3C).

Next, we determined whether mutation of either serine 61 or serine 78 to alanine abolished recognition of mouse BID by the phosphospecific antibodies. These experiments were performed in HeLa cells transfected with either wtBID, the BID-S61A mutant, or the BID-S78A mutant. The anti-pS61 and anti-pS78 antibodies recognized BID in cells expressing wtBID and treated with Etop, but not in cells expressing the BID-S61A or BID-S78A mutant, respectively (Figure S2A).

To determine if ATM (and possibly ATR) could directly phosphorylate BID, we performed in vitro kinase assays using flag-tagged human ATM and ATR (and the kinase-inactive forms) and purified recombinant mouse wtBID and the BID-S61A/S78A double mutant. Wild-type but not kinase-inactive human ATM and ATR efficiently phosphorylate recombinant wtBID in vitro, whereas mutating both S61 and S78 completely abolished BID phosphorylation (Figure S2B). Taken together, these data indicate that BID is a substrate of both ATM and ATR in vitro and that S61 and/or S78 are the sites phosphorylated by these kinases.

To determine whether BID is phosphorylated in another cell type, we have examined the phosphorylation status of BID in mouse splenocytes either not treated or treated with Etop. As shown in Figure S2C, Etop induces the phosphorylation of BID on both S61 and S78 in splenocytes.

As mentioned above, human BID carries only one PIKK consensus site (S78; Figure 3A). To determine whether endogenous human BID is phosphorylated on S78, we performed Western blot analysis with anti-human BID and anti-pS78 antibodies on lysates of HEK293 cells either not treated or treated with Etop. The anti-pS78 antibodies recognized a band of the size of human BID only in cells treated with Etop (Figure S2D). To confirm these results, we cloned human BID, generated a human BID-S78A mutant, and expressed either the wild-type or the mutant BID in HeLa cells. Western blot analysis using anti-pS78 antibodies showed an increase in the intensity of the band that represents phosphorylated BID in cells transfected with wild-type human BID but not in cells transfected with

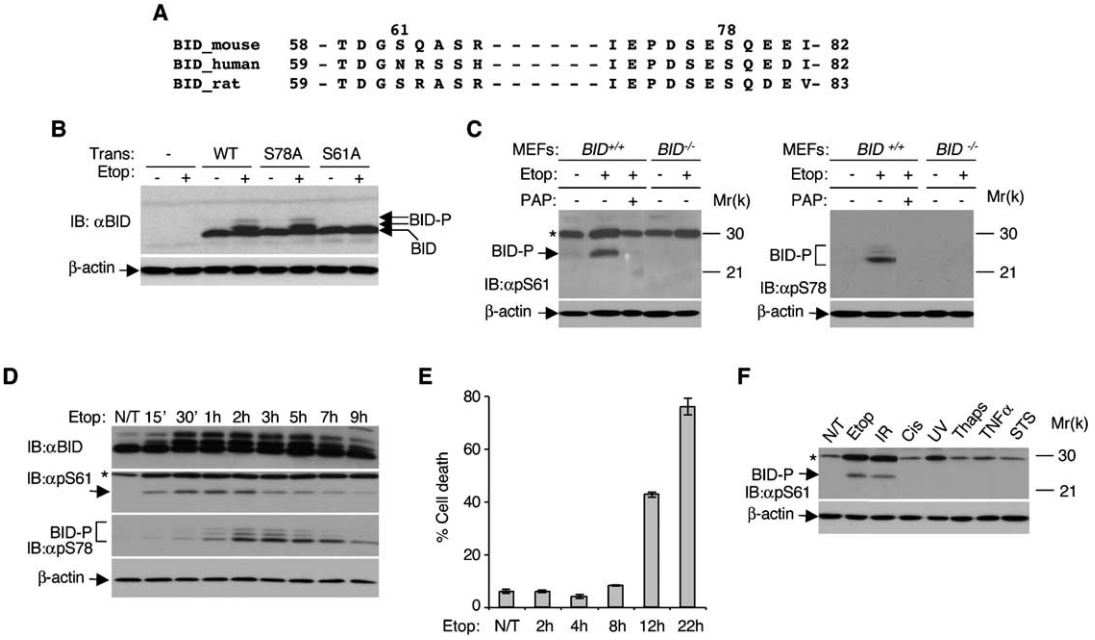

Figure 3. Mouse BID Is Phosphorylated on Serine 61 and Serine 78

(A) Mouse BID carries two PIKK consensus sites ($S^{61}Q$ and $S^{78}Q$), whereas human and rat BID carry only one ($S^{78}Q$).

(B) Mutation of serine 61 to alanine abolishes the Etop-induced double electrophoretic mobility shift in BID. HeLa cells were transiently transfected with pcDNAIII-wtBID, pcDNAIII-BID-S61A, pcDNAIII-BID-S78A or left untransfected (–). Eighteen hours posttransfection, cells were either left untreated (–) or treated with 100 μM Etop for 30 min, collected, lysed, and Western blot analyzed using anti-BID Abs. The blot was stripped and reprobed with anti-β-actin Abs to control for loading (lower panel).

(C) The phosphospecific antibodies to serine 61 and serine 78 recognize endogenous BID in MEFs treated with Etop. *BID*$^{+/+}$ or *BID*$^{-/-}$ MEFs were either left untreated (–) or treated with 100 μM Etop for 30 min (+), lysed, and Western blot analyzed using the phosphospecific Abs to either S61 (left) or S78 (right). Alternatively, *BID*$^{+/+}$ MEFs treated with 100 μM Etop for 30 min were collected, treated with potato acid phosphatase (PAP; +) for 30 min at 37°C, lysed and Western blot analyzed as above. The blots were stripped and reprobed with anti-β-actin Abs to control for loading (lower panels). BID-P marks the phosphorylated form of BID. * marks a crossreactive band.

(D) Time course of Etop-induced phosphorylation of endogenous mouse BID on S61 and S78. *BID*$^{+/+}$ MEFs were either left untreated (N/T) or treated with 100 μM Etop, collected at the indicated time points, lysed, and equal amounts of protein (20 μg per lane) were subjected to SDS-PAGE followed by Western blot analysis using either anti-BID (top), anti-pS61 (middle top), or anti-pS78 (middle bottom) Abs. The blot was stripped and reprobed with anti-β-actin Abs to control for loading (bottom). * marks a crossreactive band.

(E) Time course of Etop-induced apoptosis of MEFs. *BID*$^{+/+}$ MEFs were treated with 100 μM Etop, collected at the indicated time points, and cell death was monitored as described in the Experimental Procedures.

(F) Mouse BID is phosphorylated on S61 only in response to reagents that induce double-strand breaks in DNA. *BID*$^{+/+}$ MEFs were either left untreated (N/T) or treated with the death stimuli indicated in Figure 2A. Cells were collected 1 hr later, lysed, and equal amounts of protein (20 μg per lane) were subjected to SDS-PAGE followed by Western blot analysis using anti-pS61 Abs (top). The blot was stripped and reprobed with anti-β-actin Abs to control for loading (bottom). * marks a crossreactive band.

the BID-S78A mutant (Figure S2E). Thus, human BID is phosphorylated on S78 in response to Etop.

Phosphorylation of Serine 61 and Serine 78 Is Transient, ATM Dependent, and Only Occurs in Response to Reagents that Induce Double-Strand Breaks

To determine the time course of endogenous mouse BID phosphorylation, *BID*$^{+/+}$ MEFs were treated with Etop and Western blot analyzed with the anti-BID, the anti-pS61, or the anti-pS78 antibodies. Phosphorylation of S61 was detected by 15 min (the first time point analyzed), reached a peak at 1 hr, and was reduced by 3 hr post-Etop treatment (Figure 3D). Phosphorylation of S78 was also transient (peak at 2–3 hr), though was somewhat delayed, compared to phosphorylation of the S61 site.

Next, we determined when apoptosis began in MEFs treated with Etop and found that the onset of apoptosis occurred between 8 and 12 hr following Etop treatment (Figure 3E). Thus, BID phosphorylation occurs many hours prior to the onset of apoptosis.

To determine whether endogenous mouse BID is phosphorylated on S61 and S78 in an ATM-dependent manner, we utilized the phosphospecific antibodies for Western blot analysis of *ATM/ARF* double-knockout and *Atm*$^{+/+}$*Arf*$^{-/-}$ mouse embryonic fibroblasts either not treated or treated with Etop. This analysis demonstrated that endogenous mouse BID is phosphorylated on S61 and S78 only in *Atm*$^{+/+}$*Arf*$^{-/-}$ MEFs treated with Etop (Figure S3A).

To show that phosphorylation of mouse BID was specific for reagents inducing double-strand breaks, we treated mouse embryonic fibroblasts with several DNA-damaging and other apoptotic reagents (previously described in Figure 2). Posttreatment, cells were lysed,

and the phosphorylation of endogenous mouse BID was examined by Western blot analysis using anti-pS61 antibodies. The results demonstrated that mouse BID is phosphorylated on S61 only in response to reagents that induce double-strand breaks (Figure 3F).

Finally, to define whether phosphorylation of human BID was also ATM-dependent and occurred only in response to reagents that induce double-strand breaks, we took advantage of a stable HEK293 cell line in which ATM was knocked down by siRNA (these cells were generated like the HeLa ATM knocked-down cells [Elkon et al., 2005]). These cells and the control cells, which carried a siRNA against LacZ, were exposed to Etop, IR, UV, or STS, and Western blot analyzed using anti-pS78 antibodies. Exposure of LacZ knocked down cells to Etop or IR, but not to UV or STS, induced phosphorylation of endogenous human BID on serine 78, which did not occur in the ATM knocked-down cells (Figure S3B).

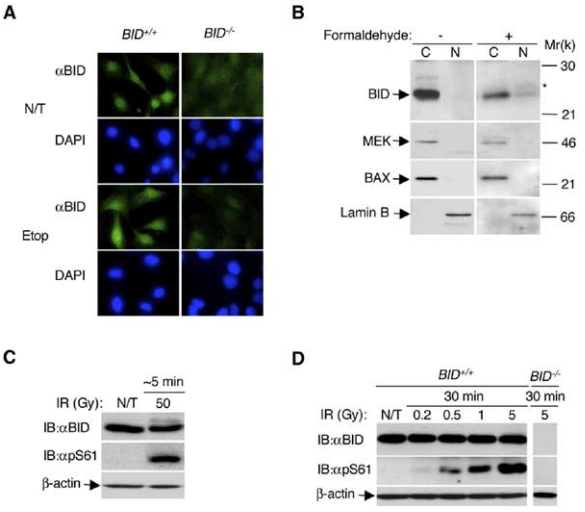

Figure 4. Mouse BID Is Partially Localized to the Nucleus, and Its Phosphorylation Occurs Very Rapidly, in Response to Extremely Low, Nonapoptotic Levels of Ionizing Radiation

(A) Positive staining of BID in the nucleus of healthy MEFs. *BID*$^{+/+}$ MEFs (left) or *BID*$^{-/-}$ MEFs (right) grown on glass coverslips, were either left untreated (top four panels) or treated with 100 μM Etop for 3 hr (bottom four panels), fixed, and immunostained with anti-BID Abs (green), as described in the Experimental Procedures. The nuclei were visualized by DAPI staining (blue).

(B) A small fraction of cellular BID is detected in the nuclear fraction. *BID*$^{+/+}$ MEFs were either left untreated (–) or treated with formaldehyde (+) and subfractionated as described in the Experimental Procedures. Aliquots of the cytosolic (C) and nuclear (N) fractions were subjected to SDS-PAGE followed by Western blot analysis using anti-BID (top), anti-MEK (middle top), anti-BAX (middle bottom), and anti-lamin B (bottom) Abs. * marks a crossreactive band that might represent a modified form of BID.

(C) Phosphorylation of BID occurs very rapidly following IR. *BID*$^{+/+}$ MEFs were either left untreated (N/T) or treated with 50 Gy IR, collected 5 min later, and lysed. Equal amounts of protein (20 μg per lane) were subjected to SDS-PAGE followed by Western blot analysis using either anti-BID Abs (top) or anti-pS61 Abs (middle). The blot was stripped and reprobed with anti-β-actin Abs to control for loading (bottom).

(D) Phosphorylation of BID occurs in response to extremely low, nonapoptotic levels of IR. *BID*$^{+/+}$ or *BID*$^{-/-}$ MEFs were either left untreated (N/T) or treated with the indicated doses of IR, collected 30 min later, lysed, and analyzed as described in (C).

Cellular BID Partially Localizes to the Nucleus, and Its Phosphorylation Occurs Very Rapidly, in Response to Extremely Low, Nonapoptotic Levels of Ionizing Radiation

Next, we analyzed the cellular location of BID and its phosphorylated form. To determine the location of BID in healthy cells, we performed immunofluoresence studies with *BID*$^{+/+}$ and *BID*$^{-/-}$ MEFs using anti-BID antibodies. Surprisingly, in these studies we obtained positive staining of BID in the nucleus (Figure 4A, left top panels). These antibodies specifically recognized BID, since we obtained very low staining in *BID*$^{-/-}$ MEFs (Figure 4A, right top panels). To determine whether Etop treatment leads to a change in the staining pattern of BID, *BID*$^{+/+}$ and *BID*$^{-/-}$ MEFs were treated with Etop for 3 hr prior to fixation. These studies have indicated that Etop did not change the staining pattern of BID (Figure 4A, bottom panels).

To assess whether BID indeed localizes to the nucleus in healthy MEFs, we have performed subcellular fractionations followed by Western blotting using anti-BID antibodies. In these experiments, cellular BID was detected only in the soluble/cytoplasmic fraction (Figure 4B, left top panel). MEK and BAX (cytosolic proteins) and lamin B (a nuclear protein) were used as markers to confirm the purity of the nuclear/cytoplasmic fractions (Figure 4B, left bottom panels). These results, together with the immunofluoresence results, suggested that BID might be loosely associated with the nuclear fraction and that cellular disruption leads to its dissociation from this fraction. To examine this possibility, cells were treated with formaldehyde as a crosslinker prior to cellular disruption. These experiments demonstrated that a small fraction of cellular BID was localized to the nuclear fraction (Figure 4B, right panels). These results suggest that BID is loosely associated with the nuclear fraction by interaction with another protein(s) and that crosslinking is required to preserve this interaction. To determine whether Etop treatment leads to a change in the levels of nuclear BID, cells were treated with Etop for 1 and 3 hr and then treated with formaldehyde followed by subcellular fractionation. We found that Etop did not change the levels of BID associated with the nuclear fraction (data not shown).

To determine the cellular location of the phosphorylated forms of BID, we performed immunofluoresence studies with the phosphospecific antibodies using *BID*$^{+/+}$ and *BID*$^{-/-}$ MEFs either not treated or treated with Etop for 30 min. These antibodies detected an increase in nuclear fluorescence in *BID*$^{+/+}$ MEFs treated with Etop; however, a similar increase was detected in *BID*$^{-/-}$ MEFs (data not shown). Thus, these antibodies crossreact with other phospho-S/T-Q proteins. Nonetheless, the fact that BID partially localizes to the nucleus and that all currently identified substrates of ATM are nuclear proteins, suggests that BID is phosphorylated in the nucleus.

To assess whether BID might be involved in the immediate cellular response to DNA damage, we next

determined the earliest point at which BID in mouse embryonic fibroblasts was phosphorylated, following exposure to ionizing radiation. Phosphorylation of serine 61 was detectable immediately after exposing cells to 50 Gy IR (Figure 4C).

We previously determined that phosphorylation of BID on both serine 61 and serine 78 occurs several hours prior to the onset of apoptosis (Figure 3). We therefore speculated that phosphorylation might also occur in response to extremely low levels of ionizing radiation which do not result in apoptosis. Indeed, we determined that a 25-fold lower dose of IR (0.2 Gy) was sufficient to induce phosphorylation of BID (Figure 4D).

BID$^{-/-}$ Mouse Embryonic Fibroblasts Fail to Accumulate in the S and G_2 Phases of the Cell Cycle Following Etoposide Treatment

The functional consequences of certain ATM phosphorylation events include activation of cell cycle checkpoints, which result in temporary arrest of cell cycle progression to enable DNA repair (Iliakis et al., 2003). The best-documented, damage-induced cell cycle checkpoints operate in the G_1/S boundary and at the S and G_2 phases. To examine the possible involvement of BID in cell cycle arrest following DNA double-strand breaks, we performed cell cycle analyses on *BID*$^{+/+}$ and *BID*$^{-/-}$ mouse embryonic fibroblasts either not treated or treated with etoposide. Etop induced accumulation of *BID*$^{+/+}$ MEFs in the S and G_2 phases of the cell cycle (as measured 8 hr after release into drug-free medium), whereas such an accumulation was not observed in the *BID*$^{-/-}$ MEFs (Figure 5A). These results suggest that BID is important for the accumulation of cells in the S and G_2 phases of the cell cycle following double-strand break DNA damage.

To determine whether BID is required for S phase arrest following DNA damage, we performed double-labeling experiments with BrdU and PI to determine the level of DNA synthesis and to follow the progress of cells through S phase after Etop treatment. The results demonstrate that *BID*$^{+/+}$ MEFs show a decrease in DNA synthesis (less BrdU-positive cells), whereas *BID*$^{-/-}$ MEFs fail to show a decrease in DNA synthesis (Figure 5B). Moreover, *BID*$^{-/-}$ MEFs are not delayed in their progression form S to G_2/M (Figure 5C). Taken together, these experiments prove that *BID*$^{-/-}$ MEFs fail to arrest in S phase following Etop treatment.

BID$^{-/-}$ Mouse Embryonic Fibroblasts Expressing a Nonphosphorylatable BID Mutant (S61A/S78A) Do Not Accumulate in the S Phase Following Etoposide Treatment

To assess whether ATM-mediated phosphorylation is regulating BID's function in this process, we generated *BID*$^{-/-}$ single stable clones expressing either wtBID or a nonphosphorylatable BID mutant (S61A/S78A). We initially confirmed that wtBID (in the wtBID clones) was phosphorylated on S61 and S78 in response to Etop and that BID-S61A/S78A (in the mutant BID clones) was not (Figure 6A).

Next, we performed cell cycle analysis on two of the wtBID and two of the BID-S61A/S78A stable clones. As shown in Figure 6B, Etop induced accumulation of the wtBID clones in the S and G_2 phases of the cell cycle (as measured 8 hr after release into drug-free medium), whereas the mutant BID clones bypassed accumulation in the S phase and rapidly accumulated in the G_2 phase. Thus, the mutant BID cells were found to be impaired in their ability to temporarily arrest in S phase following double-strand break DNA damage.

BID$^{-/-}$ Mouse Embryonic Fibroblasts Expressing BID-S61A/S78A Are More Susceptible to Etop-Induced Apoptosis Than Those Expressing Wild-Type BID

To explore a possible connection between BID phosphorylation, cell cycle progression, and apoptosis, we assessed the levels of apoptosis in the two wtBID and in the two BID-S61A/S78A clones either not treated or treated with Etop. Our results indicated that Etop induced a significantly higher rate of apoptosis in *BID*$^{-/-}$ clones expressing BID-S61A/S78A than in the *BID*$^{-/-}$ clones expressing wtBID (Figure 7A). It is interesting that UV or TNFα treatment did not induce increased apoptosis in the mutant BID clones (Figure 7A). Western blot analysis using anti-BID antibodies indicated that the increase in apoptosis seen in the mutant BID clones in response to Etop was not due to either higher levels of expression of mutant BID or to its enhanced cleavage to tBID (Figure 7B). Thus, the mutant BID clones were found to be more susceptible to apoptotsis induced solely by a reagent that leads to DNA double-strand breaks.

Discussion

In the present study, we demonstrated that double-strand break DNA-damaging reagents induced an immediate and transient phosphorylation of BID. In addition, we showed that this phosphorylation was mediated by the ATM kinase. Most importantly, we demonstrated that *BID*$^{-/-}$ mouse embryonic fibroblasts failed to delay the cell cycle in response to etoposide and that introduction of a nonphosphorylatable BID mutant restored delay in the G_2 but not in the S phase. Moreover, in response to etoposide, the mutant BID cells entered apoptosis more readily than did the wild-type BID cells.

Previously, we suggested that full-length BID is a player in the DNA-damage pathway, since a caspase-8 noncleavable BID mutant sensitized *BID*$^{-/-}$ mouse embryonic fibroblasts to DNA damage-induced apoptosis (Sarig et al., 2003). Our current findings demonstrate that in MEFs, BID is important for apoptosis induced by a variety of DNA-damaging reagents (Figure 1). Splenocytes from *BID*$^{-/-}$ mice also display less susceptibility to DNA damage, indicating that the decreased death response to DNA damage is a general feature of BID deficiency.

As mentioned above, *BID*$^{-/-}$ MEFs are less susceptible than *BID*$^{+/+}$ MEFs to reagents that induce different forms of DNA damage (Figure 1). On the other hand, BID phosphorylation occurs only in response to reagents that induce double-strand breaks in DNA. Thus, phosphorylation of BID does not seem to be critical for its proapoptotic activity. However, lack of BID phosphorylation does effect the susceptibility of cells to

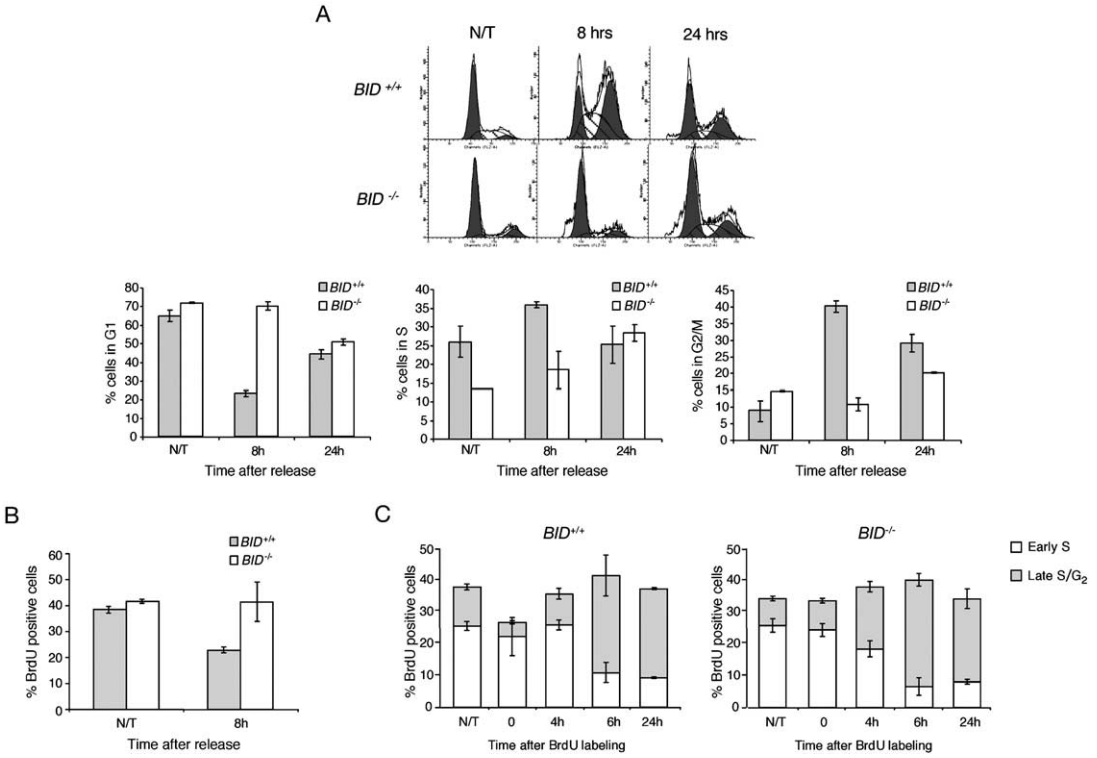

Figure 5. *BID*$^{-/-}$ Mouse Embryonic Fibroblasts Fail to Arrest in the S Phase of the Cell Cycle Following Etoposide Treatment

(A) *BID*$^{-/-}$ mouse embryonic fibroblasts do not accumulate in the S and G_2 phases of the cell cycle following etoposide treatment. *BID*$^{+/+}$ or *BID*$^{-/-}$ MEFs were either left untreated (N/T) or treated with 20 μM Etop for 2 hr, rinsed, and then released into drug-free medium. At the indicated time points, the DNA content was analyzed by flow cytometry as described in the Experimental Procedures. The actual raw data from a representative experiment together with multiline plots generated by the ModFit LT computer software program appear in the top panels. The dark histograms represent the percent of cells in the G_1 and G_2/M phases, and the hatched histograms represent the percent of cells in S phase. The exact percentage of cells in each phase of the cell cycle is shown in the bottom three panels. The data represent the means ±SEM of pooled results from three independent experiments.

(B) *BID*$^{-/-}$ mouse embryonic fibroblasts fail to decrease DNA synthesis following Etop treatment. *BID*$^{+/+}$ or *BID*$^{-/-}$ MEFs were either left untreated (N/T) or treated with 20 μM Etop for 2 hr, rinsed, and then released into drug-free medium. Eight hours after release, cells were pulse-labeled with BrdU for 30 min to determine DNA synthesis. The percentage of BrdU-positive cells was determined as described in the Experimental Procedures. The data represent the means ±SEM of pooled results from three independent experiments.

(C) *BID*$^{-/-}$ mouse embryonic fibroblasts are not delayed in their progression from S to G_2/M following Etop treatment. *BID*$^{+/+}$ (left) or *BID*$^{-/-}$ (right) MEFs were either left untreated (N/T) or treated with 20 μM Etop for 2 hr and labeled with BrdU for 30 min. Cells were then rinsed, incubated in fresh medium for the indicated time periods, and fixed. The percentage of BrdU-positive cells in early S phase and in late S/G_2 phase was determined as described in the Experimental Procedures. The data represent the means ±SEM of pooled results from three independent experiments.

double-strand break DNA damage since *BID*$^{-/-}$ MEFs expressing the BID-S61A/S78A mutant are more susceptible than *BID*$^{-/-}$ MEFs expressing wild-type BID to etoposide-induced apoptosis (Figure 7). Thus, ATM-mediated BID phosphorylation might serve as a mechanism to inhibit BID's apoptotic activity or alternatively as a mechanism to activate a prosurvival activity of BID.

If phosphorylation were inhibiting the apoptotic activity of BID, then what would likely be the molecular basis of such inhibition? The only known apoptotic function of BID lies in its ability to induce the release of proapoptotic factors from the mitochondria (e.g., cytochrome c). Caspase-truncated BID (tBID) is much more efficient than full-length BID in inducing cytochrome c release; it would therefore be expected that ATM-mediated BID phosphorylation inhibits the cleavage of BID, since casein kinase 1 and/or 2-mediated phosphorylation of BID was demonstrated to inhibit its cleavage (Desagher et al., 2001).

However, our findings suggest that ATM-mediated phosphorylation of BID is not related to BID cleavage, for the following reasons: phosphorylation occurs many hours before the activation of caspases and the onset of apoptosis (Figure 3 and data not shown). A relatively small amount of BID is phosphorylated (Figure 2), and phosphorylation occurs also in response to extremely low, nonapoptotic levels of DNA damage (Figure 4). Moreover, the BID-S61A/S78A mutant was not found to be more susceptible to cleavage than was wtBID (Figure 7). Lastly, though TNFα relies on the generation of tBID to induce/enhance apoptosis (Yin et al., 1999; Zhao et al., 2001), the BID-S61A/S78A mutant clones are not more susceptible to TNFα-induced apoptosis than are the wtBID clones (Figure 7). Thus, BID phos-

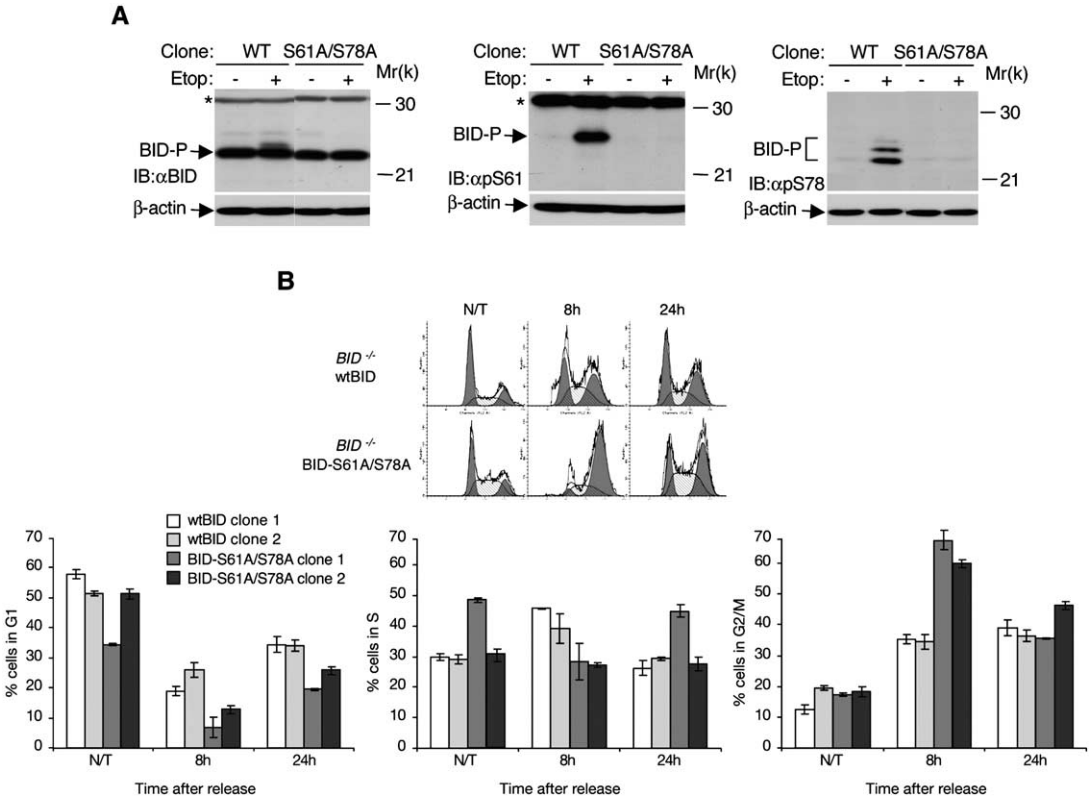

Figure 6. *BID*$^{-/-}$ MEFs Expressing a Nonphosphorylatable BID Mutant (S61A/S78A) Do Not Accumulate in the S Phase Following Etop Treatment

(A) BID-S61A/S78A expressed in *BID*$^{-/-}$ MEFs is not recognized by the phosphospecific Abs. *BID*$^{-/-}$ MEFs stably expressing either wtBID or the BID-S61A/S78A mutant were treated with 20 μM Etop for 1 hr, lysed, and equal amounts of protein (20 μg per lane) were subjected to SDS-PAGE, followed by Western blot analysis using either anti-BID Abs (left panel) or the phosphospecific Abs (middle and right panels). The blots were stripped and reprobed with anti-β-actin Abs to control for loading (lower panels). * mark crossreactive bands.

(B) *BID*$^{-/-}$ MEFs stably expressing BID-S61A/S78A do not accumulate in the S phase following Etop treatment. *BID*$^{-/-}$ MEFs stably expressing either wtBID or BID-S61A/S78A (two clones from each) were treated with 20 μM Etop for 2 hr, rinsed, and then released into drug-free medium. At the times indicated, the DNA content was analyzed by flow cytometry as described in the Experimental Procedures. The actual raw data from a representative experiment together with multiline plots generated by the ModFit LT computer software program appear in the top panel. The dark histograms represent the percent of cells in the G_1 and G_2/M phases, and the hatched histograms represent the percent of cells in S phase. The exact percentage of cells in each phase of the cell cycle (in each of the four clones) is shown in the bottom three panels. The data represent the means ±SEM of pooled results from three independent experiments.

phorylation does not seem to serve as a mechanism to inhibit BID's apoptotic activity.

The results presented in Figures 5 and 6 suggest that ATM-mediated phosphorylation of BID regulates a novel, prosurvival function of BID related to cell cycle arrest following DNA double-strand breaks. We first found that etoposide induced accumulation of *BID*$^{+/+}$ mouse embryonic fibroblasts in the S and G_2 phases of the cell cycle, whereas such an accumulation was not observed in the *BID*$^{-/-}$ MEFs (Figure 5). Moreover, using BrdU labeling, we have demonstrated that BID is specifically required for S phase arrest. We then reintroduced wild-type BID into *BID*$^{-/-}$ cells and found that this addition restored the ability to accumulate in the S and G_2 phases of the cell cycle. Introducing the nonphosphorylatable BID mutant into *BID*$^{-/-}$ cells, however, restored accumulation only in the G_2 phase (Figure 6). These findings imply that BID phosphorylation plays an important role in S phase arrest.

To demonstrate the BID-dependent S phase checkpoint, we have used relatively high levels of etoposide, suggesting that this function of BID is associated with high levels of genotoxic stress in fibroblasts. On the other hand, in myeloid and in activated T cells, this function of BID is associated with lower levels of genotoxic stress (Zinkel et al., 2005 [this issue of *Cell*]). Hematopoietic cells are primed to undergo cell cycle arrest and apoptosis following treatment with DNA-damaging reagents, whereas fibroblasts are relatively resistant to DNA-damaging reagents and prevent proliferation of mutations by entering into long-term G_1 or G_2 arrest (Baus et al., 2003; Di Leonardo et al., 1994). Thus, the activation threshold and the biological impact of the BID-dependent S phase checkpoint function may vary largely among different cell types.

How might the involvement of BID in S phase arrest be related to apoptosis? Following DNA double-strand breaks, the cell may decide to activate a survival system (mainly through the ATM kinase, which induces cell cycle arrest and DNA repair), or in the face of extensive

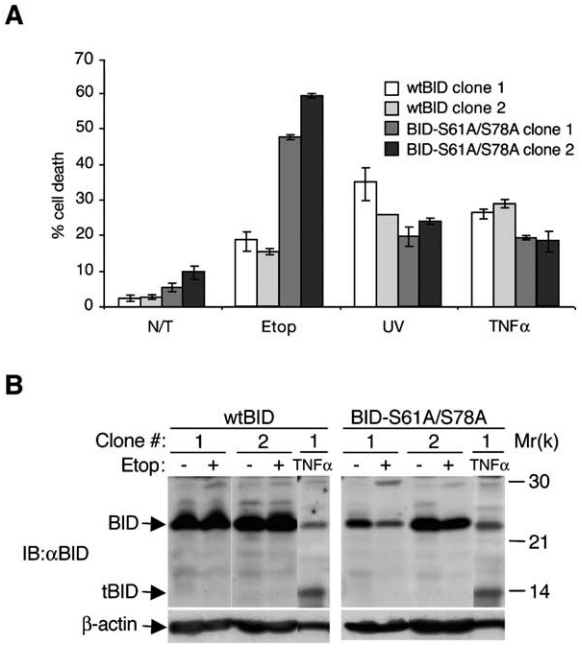

Figure 7. *BID*$^{-/-}$ Mouse Embryonic Fibroblasts Expressing BID-S61A/S78A Are More Susceptible to Etop-Induced Apoptosis Than Those Expressing Wild-Type BID

(A) *BID*$^{-/-}$ MEFs stably expressing either wtBID or BID-S61A/S78A (the four clones shown in Figure 6) were either left untreated (N/T) or treated with Etop (50 μM; 18 hr), UV (20 J/m^2; 24 hr), or TNFα (40 ng/ml together with 2 μg/ml actinomycin D; 4.5 hr). Cell death was monitored by FACScan using PI dye exclusion, as described in the Experimental Procedures. The data represent the means ±SEM of pooled results from three independent experiments.

(B) The enhanced death obtained with the BID-S61A/S78A clones is not due to higher expression of mutant BID or to more cleavage to tBID. The two wtBID and two mutant BID clones were treated either with 50 μM Etop for 18 hr or with TNFα/ActD for 4.5 hr, lysed, and equal amounts of protein (20 μg per lane) were subjected to SDS-PAGE, followed by Western blot analysis using anti-BID Abs. For the TNFα treatment, only clones #1 are shown. The blots were stripped and reprobed with anti-β-actin Abs to control for loading (lower panels).

or irreparable damage, the cell may activate the apoptotic machinery. The results presented in Figure 7 demonstrate that *BID*$^{-/-}$ MEFs expressing the BID-S61A/S78A mutant are more susceptible than *BID*$^{-/-}$ MEFs expressing wild-type BID to etoposide-induced apoptosis, but not to UV- or to TNFα-induced apoptosis. Thus, it appears that the nonphosphorylatable BID mutant sensitizes *BID*$^{-/-}$ MEFs to apoptotsis induced only by reagents that induce double-strand breaks in DNA. These results, together with the cell cycle results (Figures 5 and 6) suggest that the impaired ability of the mutant BID cells to induce cell cycle arrest results in increased sensitivity to double-strand break DNA damage.

If BID is indeed capable of playing a prosurvival role in the response of cells to DNA double-strand breaks, then why are the *BID*$^{-/-}$ MEFs less sensitive than *BID*$^{+/+}$ MEFs to apoptosis induced by etoposide and ionizing radiation (Figure 1)? BID may play both a prosurvival and a proapoptotic role in this pathway. Based on our finding that the phosphorylation of BID occurs in response to extremely low levels of ionizing radiation and increases in an ionizing radiation dose-dependent manner (Figure 4), we propose that BID acts as a sentinel of DNA double-strand breaks. BID might translate the damage into either cell cycle arrest/DNA repair processes (at low levels of damage) or apoptosis (at high levels of damage).

In summary, this study raises the novel possibility that the BH3-only BID protein, a molecule that was previously considered to be active only as a proapoptotic factor, may also play a prosurvival role. If BID is indeed playing both a proapoptotic and a prosurvival function in the DNA-damage pathway, then it is an excellent candidate to link DNA repair processes and apoptosis.

Experimental Procedures

Mouse Embryonic Fibroblasts

BID$^{-/-}$ mice (originally kept on a mixed C57BL/6 × 129S background) had been bred to wt C57BL/6 mice 12 times in order to obtain animals that are F12 on a C57BL/6 background. *BID*$^{-/-}$ MEFs were generated from the F12 mice. *BID*$^{+/+}$ and *BID*$^{-/-}$ primary MEFs were prepared from 11- to 13-day-old embryos and maintained in ISCOVE's medium containing 10% fetal bovine serum (MEF medium). *ATM/ARF* double-knockout and *Atm*$^{+/+}$*Arf*$^{-/-}$ MEFs were obtained from Chuck J. Sherr (St. Jude Children's Research Hospital).

Cell Viability Assays

Cell viability was determined by propidium iodide (PI) dye exclusion. PI (25 μg/ml) was added to the cells immediately prior to analysis by FACScan (Beckton Dickinson).

Cell Cycle Assays

MEFs were treated with 20 μM Etop for 2 hr, rinsed, and then released into drug-free medium. Eight or twenty-four hours after release, cells were collected for fixation in methanol. Following fixation, cells were washed and resuspended in PBS with 25 μg/ml PI and 50 μg/ml RNase a half-hour before FACScan analysis. Analysis of the cell cycle results was performed using the ModFit LT program (Tripathi et al., 2003).

Generation of Phosphospecific Antibodies

Anti-pS61 and anti-pS78 were generated in collaboration with Bethyl Laboratories, Inc. Briefly, immunogens were phosphorylated synthetic peptides, which represented portions of mouse BID around either serine 61 or serine 78. Antibodies that were not phosphospecific were removed by solid phase absorption. Antibodies that were specific for either BID pSer61 or BID pSer78 were affinity-purified using the phosphopeptide immobilized on solid support.

Supplemental Data

Supplemental Data include three figures and Supplemental Experimental Procedures and can be found with this article online at http://www.cell.com/cgi/content/full/122/4/593/DC1/.

Acknowledgments

I dedicate this paper to Stanley J. Korsmeyer, an extraordinary scientist, mentor, and person, who contributed enormously to the development of my career. We are grateful to Yosef Shiloh for reagents, discussions, and comments on the manuscript. We would also like to thank Doron Ginsberg, Yosef Shaul, and Moshe Oren for stimulating discussions and comments on the manuscript, Reuven Agami for sharing unpublished results, and Ami Navon for help with producing the recombinant proteins. ATM wt and KI cDNA were a kind gift from Michael Kastan (St. Jude's Cancer Center), and ATR wt and KI cDNA were a kind gift from Robert Abraham (The Burnham Institute). This work was supported in part by the Israel Sci-

ence Foundation, Israel Cancer Research Fund, Minerva Stiftung, the Y. Leon Benoziyo Institute for Molecular Medicine, the Willner Family Center for Vascular Biology, and Mr. and Mrs. Stanley Chais. H.N. is a recipient of the Sara Lee Schupf postdoctoral fellowship. A.G. is the incumbent of the Armour Family Career Development Chair of Cancer Research.

Received: December 31, 2004
Revised: May 3, 2005
Accepted: June 13, 2005
Published: August 25, 2005

References

Baus, F., Gire, V., Fisher, D., Piette, J., and Dulic, V. (2003). Permanent cell cycle exit in G2 phase after DNA damage in normal human fibroblasts. EMBO J. *22*, 3992–4002.

Desagher, S., Osen-Sand, A., Montessuit, S., Magnenat, E., Vilbois, F., Hochmann, A., Journot, L., Antonsson, B., and Martinou, J.C. (2001). Phosphorylation of bid by casein kinases I and II regulates its cleavage by caspase 8. Mol. Cell *8*, 601–611.

Di Leonardo, A., Linke, S.P., Clarkin, K., and Wahl, G.M. (1994). DNA damage triggers a prolonged p53-dependent G1 arrest and long-term induction of Cip1 in normal human fibroblasts. Genes Dev. *8*, 2540–2551.

Elkon, R., Rashi-Elkeles, S., Lerenthal, Y., Linhart, C., Tenne, T., Amariglio, N., Rechavi, G., Shamir, R., and Shiloh, Y. (2005). Dissection of a DNA-damage-induced transcriptional network using a combination of microarrays, RNA interference and computational promoter analysis. Genome Biol. *6*, R43.

Iliakis, G., Wang, Y., Guan, J., and Wang, H. (2003). DNA damage checkpoint control in cells exposed to ionizing radiation. Oncogene *22*, 5834–5847.

Kaina, B. (2003). DNA damage-triggered apoptosis: critical role of DNA repair, double-strand breaks, cell proliferation and signaling. Biochem. Pharmacol. *66*, 1547–1554.

Kamijo, T., van de Kamp, E., Chong, M.J., Zindy, F., Diehl, J.A., Sherr, C.J., and McKinnon, P.J. (1999). Loss of the ARF tumor suppressor reverses premature replicative arrest but not radiation hypersensitivity arising from disabled atm function. Cancer Res. *59*, 2464–2469.

Kim, S.T., Lim, D.S., Canman, C.E., and Kastan, M.B. (1999). Substrate specificities and identification of putative substrates of ATM kinase family members. J. Biol. Chem. *274*, 37538–37543.

Puthalakath, H., and Strasser, A. (2002). Keeping killers on a tight leash: transcriptional and post-translational control of the pro-apoptotic activity of BH3-only proteins. Cell Death Differ. *9*, 505–512.

Sarig, R., Zaltsman, Y., Marcellus, R.C., Flavell, R., Mak, T.W., and Gross, A. (2003). BID-D59A is a potent inducer of apoptosis in primary embryonic fibroblasts. J. Biol. Chem. *278*, 10707–10715.

Sax, J.K., Fei, P., Murphy, M.E., Bernhard, E., Korsmeyer, S.J., and El-Deiry, W.S. (2002). BID regulation by p53 contributes to chemosensitivity. Nat. Cell Biol. *4*, 842–849.

Shiloh, Y. (2003). ATM and related protein kinases: safeguarding genome integrity. Nat. Rev. Cancer *3*, 155–168.

Tripathi, A.K., Chaturvedi, R., Ahmad, R., Asim, M., Sawlani, K.K., Singh, M.K., Tripathi, P., and Tekwani, B.L. (2003). Flow cytometric analysis of aneuploidy and S-phase fraction in chronic myeloid leukemia patients: role in early detection of accelerated phase. Leuk. Res. *27*, 899–902.

Wang, X. (2001). The expanding role of mitochondria in apoptosis. Genes Dev. *15*, 2922–2933.

Wei, M.C., Zong, W.X., Cheng, E.H., Lindsten, T., Panoutsakopoulou, V., Ross, A.J., Roth, K.A., MacGregor, G.R., Thompson, C.B., and Korsmeyer, S.J. (2001). Proapoptotic BAX and BAK: a requisite gateway to mitochondrial dysfunction and death. Science *292*, 727–730.

Yin, X.M., Wang, K., Gross, A., Zhao, Y., Zinkel, S., Klocke, B., Roth, K.A., and Korsmeyer, S.J. (1999). Bid-deficient mice are resistant to Fas-induced hepatocellular apoptosis. Nature *400*, 886–891.

Zhao, Y., Li, S., Childs, E.E., Kuharsky, D.K., and Yin, X.M. (2001). Activation of pro-death Bcl-2 family proteins and mitochondria apoptosis pathway in tumor necrosis factor-alpha-induced liver injury. J. Biol. Chem. *276*, 27432–27440.

Zinkel, S.S., Hurov, K.E., Ong, C., Abtahi, F.M., Gross, A., and Korsmeyer, S.J. (2005). A role for proapoptotic BID in the DNA-damage response. Cell *122*, this issue, 579–591.